



Cite this: *Org. Biomol. Chem.*, 2025, **23**, 8755

Received 29th July 2025,
Accepted 28th August 2025

DOI: 10.1039/d5ob01223f
rsc.li/obc

Morpholino-based phosphorothioate analogs via oxathiaphospholane chemistry: synthesis, structural insights and stability

Katarzyna Jastrzębska, * Agata Szymańska, Tomasz Pawlak and Rafał Dolot

We present the application of the oxathiaphospholane method for the synthesis of novel P-stereodefined phosphorothioate N-modified morpholino analogs, showcasing its potential for creating therapeutically relevant compounds. Additionally, we provide valuable structural insights into their stereochemistry, including a detailed analysis of stereochemical configurations. We also report on the enzymatic stability of these compounds in 10% (v/v) fetal bovine serum (FBS), thereby mimicking *in vivo* conditions. These findings pave the way for further exploration of P-stereodefined nucleic acid analogs in molecular medicine and gene therapy applications.

Introduction

The morpholine (1,4-oxazinane) motif (Fig. 1) has garnered significant attention in medicinal chemistry and drug discovery due to its unique physicochemical properties and widespread application in biologically active molecules.¹ This heterocyclic structure combines an oxygen atom and a nitrogen atom within a six-membered ring, imparting stability, solubility, and biocompatibility advantages to compounds that include it. Morpholine derivatives have been utilized in diverse therapeutic areas, including antivirals,² anticancer agents,³ and central nervous system drugs.⁴ Their ability to enhance the pharmacokinetic and pharmacodynamic profiles of therapeutic agents underscores their importance in modern drug discovery.

Phosphorodiamidate morpholino oligomers (PMOs, Fig. 1)⁵ represent a notable application of the morpholine motif in the realm of antisense therapy. These synthetic analogs of nucleic acids replace the traditional sugar-phosphate backbone with a phosphorodiamidate-linked morpholine framework. This modification confers several advantages, including resistance to enzymatic degradation, improved binding specificity to target RNA, and reduced immunogenicity. As a result, PMOs are highly promising candidates for the treatment of various infectious and inherited diseases. In infectious disease therapy, PMOs have shown efficacy against viral pathogens such as influenza,⁶ Ebola,⁷ and SARS-CoV-2 viruses,⁸ as well as bacterial infections,⁹ by targeting essential mRNA sequences

and disrupting protein synthesis. In the context of inherited diseases, PMOs have been employed in exon-skipping strategies to restore functional protein expression, as demonstrated in Duchenne muscular dystrophy (DMD).¹⁰ The PMO drug eteplirsen (marketed as Exondys 51) was the first approved therapy for DMD, showcasing the clinical potential of this technology. Recently, Caruthers' lab developed a method for synthesizing thiomorpholino oligonucleotides (TMOs)¹¹ using phosphoramidite chemistry. TMOs, featuring a phosphorothioate (PS) group and a morpholine ring, have shown promise in oligotherapeutics. Studies by Dumbović *et al.* and Le *et al.* highlight their intriguing biological properties and therapeutic potential.^{12,13}

Many studies show that stereoisomerically pure PS oligonucleotides exhibit enhanced efficacy both *in vitro* and *in vivo* compared to diastereomeric mixtures. For example, work by Iwamoto *et al.*¹⁴ demonstrated that stereopure phosphorothioate oligonucleotides display improved stability and target

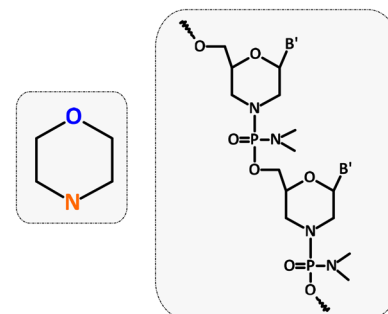


Fig. 1 Schematic representation of the morpholino ring (left) and PMO (right).



affinity, leading to better therapeutic outcomes in gene silencing applications. The ongoing development of stereopure PS oligonucleotides in clinical settings emphasizes the critical role of stereochemistry in advancing the field of oligonucleotide therapeutics.¹⁵

The growing interest in the stereocontrolled synthesis of phosphorothioate analogs has driven the development of various methods, including the pioneering approach by Stec,^{16,17} which utilizes P-diastereomerically pure monomers containing the 2-thio-1,3,2-oxathiaphospholane moiety. This oxathiaphospholane (OTP) method has already been successfully applied to the stereocontrolled synthesis of a wide range of phosphorothioate analogs, including PS-DNA, PS-LNA,^{18,19} PS-GNA,²⁰ PS-RNA, and PS-(2'-OMe) RNA.²¹ It has also been used for the preparation of NPS-oligos,²² which combine the advantageous features of phosphorothioates (PS) and NPO-oligos. NPO-oligos were originally proposed by Gryaznov *et al.*, who described oligo(deoxyribonucleoside phosphoramidates)²³ in which the 3'-oxygen atom is replaced with nitrogen. These compounds exhibit high nucleolytic stability and adopt A-like duplex conformations, contributing to enhanced thermal stability. Notably, NPO-oligos have also demonstrated biological activity, including allosteric inhibition of telomerase.²⁴

Building on this foundation, the 1,3,2-oxathiaphospholane (OTP) method²⁵ was modified to enable the preparation of P-stereodefined morpholino phosphorothioate analogs²⁶ (Fig. 2b), further advancing the field. To further our research on the design and synthesis of modified nucleic acid fragments as potential therapeutic and diagnostic tools, we have synthesized a new series of P-diastereomerically pure oxathiaphospholane derivatives of N-modified morpholino nucleosides (mB'-NOTP, Fig. 2c).

This article outlines the use of the oxathiaphospholane method for the synthesis of P-stereodefined phosphorothioate N-modified morpholino analogs (Fig. 3). We describe the synthesis and HPLC separation of oxathiaphospholane derivatives of N-modified morpholino nucleosides (2) into pure P-diastereomers (fast- and slow-eluting), and one of these monomers was successfully crystallized. X-ray crystallographic analysis of **4a**^{Fast} confirmed the absolute *S_P* configuration at the phosphorus center. These P-diastereomerically pure monomers were subsequently used in the synthesis of

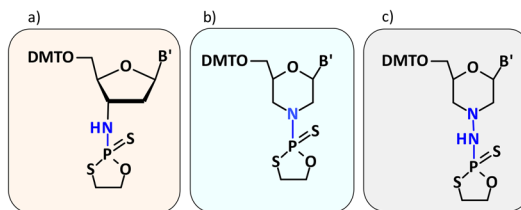


Fig. 2 Schematic representation of oxathiaphospholane derivatives of 3'-amino-2',3'-dideoxyribo- (a),²² morpholino- (b),²⁶ and N-aminomorpholino nucleosides (c, this study).

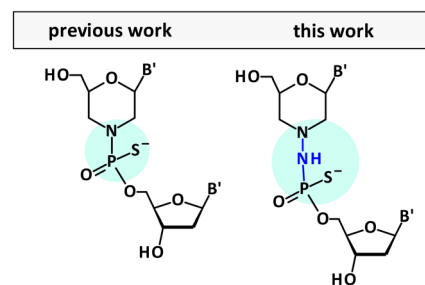


Fig. 3 Schematic representation of P-stereodefined dinucleoside 3',5'-phosphorothioates with morpholino (left) and *N*-amino morpholino (right) modifications.

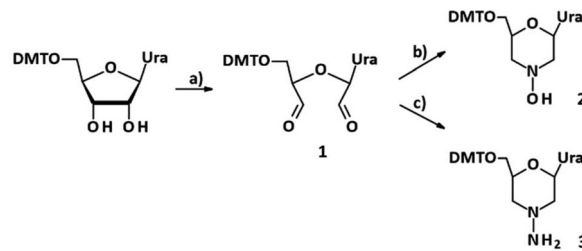
P-stereodefined dinucleotides and subjected to stability evaluation.

Results and discussion

Preparation of N-modified morpholino nucleosides (2 and 3)

We have successfully synthesized N-modified morpholino nucleosides using an optimized approach. Notably, the procedures described in the literature required modification to achieve the desired results.²⁷

The first step involved oxidative ring cleavage of the vicinal diol unit of uridine, yielding a dialdehyde intermediate (**1**). This was followed by cyclization *via* double reductive amination with suitable amines, hydroxylamine and hydrazine, to produce two different N-modified morpholinos (mU^{OH}, **2**, and mU^{NH₂}, **3**, respectively, Scheme 1). Briefly, dialdehyde (**1**) was dissolved in anhydrous methanol, followed by the sequential addition of NaHCO₃ and hydroxylamine hydrochloride. The mixture was stirred for 1 hour, after which Et₃N and NaCNBH₃ were added. Stirring was continued, and trifluoroacetic acid was introduced into the reaction mixture. After an additional 1 hour, the reaction mixture was filtered. The crude product (**2**) was purified by extraction followed by flash chromatography, affording compound **2** as a white solid in 62% yield (Fig. S3, SI).



Scheme 1 a) NaIO₄ (1.2 equiv.), anhydrous methanol; (b) 1 step: NH₂OH·HCl (2.0 equiv.), NaHCO₃ (2.0 equiv.), 2 step: NaCNBH₃ (2.0 equiv.), TFA (1.0 equiv.), anhydrous methanol; and (c) 1 step: NH₂NH₂ (2.0 equiv.), boric acid (2.0 equiv.); 2 step: NaCNBH₃ (2.0 equiv.), TFA (1.0 equiv.), anhydrous methylene chloride.

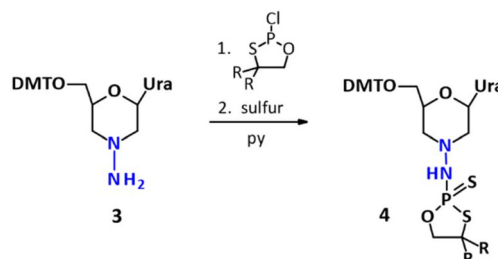
Subsequently, the synthesis of the *N*-aminomorpholino nucleoside **3** was carried out. The dialdehyde (**1**) was dissolved in methanol, followed by the addition of hydrazine and boric acid. The reaction mixture was stirred for 15 minutes, followed by the addition of sodium cyanoborohydride and trifluoroacetic acid (TFA). Stirring was continued for an additional 10 minutes, after which the reaction was quenched. The crude product was purified by extraction and flash chromatography, affording compound **3** as a white solid in 58% yield (Fig. S4, SI).

Preparation of P-diastereomerically pure oxathiaphospholane derivatives of *N*-aminomorpholino nucleosides

Next, attempts were made to synthesize a series of novel *N*-modified morpholino oxathiaphospholane derivatives. The first phosphorylation reaction of 4-hydroxymorpholino nucleoside uridine (mU^{OH} , **2**) yielded a mixture of 2-thio-1,3,2-oxathiaphospholane (**2.1**) and its oxidized analog, 2-oxo-1,3,2-oxathiaphospholane (**2.2**, Scheme 2 and Fig. S5–9, SI). This transformation is likely caused by the *in situ* formation of hypochlorous acid (HClO), a strong oxidizing agent that can be generated during the phosphorylation reaction. Despite the use of pyridine as the solvent, which typically provides a basic and protective environment, partial oxidation of the thio compound ($P=S$, **2.1**) to its oxo analog ($P=O$, **2.2**) still occurs. As a result, the $N-O-P$ bond demonstrated instability under the conditions employed in the oxathiaphospholane method.

Due to the difficulties encountered in synthesizing a morpholino-oxathiaphospholane monomer with a hydroxyl group ($mU^{O}OTP$), an alternative strategy was pursued by using a nucleoside with an amino group.

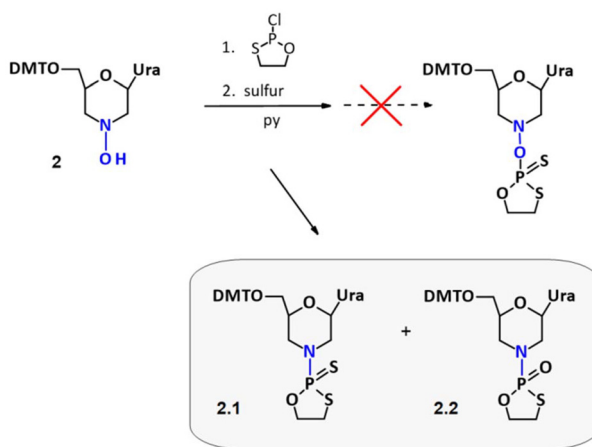
This modification proved to be more feasible, overcoming the instability issues associated with the $N-O-P$ derivative. As a result, the desired product, $mU^{N}OTP$ (**4**), was successfully synthesized with a satisfactory yield, demonstrating the potential of this adjusted methodology (Scheme 3).²⁸



Scheme 3 The synthetic route to the morpholino oxathiaphospholane (OTP) derivative $mU^{N}OTP$ (**4**). Compound **4a** corresponds to the unsubstituted derivative ($R,R = H$), while **4b** contains a pentamethylene bridge ($R,R = -(CH_2)_5-$).

The synthesis of the oxathiaphospholane monomers $mU^{N}OTP$ (**4a^{MIX}** and **4b^{MIX}**) was performed following a general procedure established for the preparation of standard OTP monomers. Briefly, the morpholino nucleosides, dried overnight to ensure the removal of residual moisture, were phosphorylated using 2-chloro-1,3,2-oxathiaphospholane (for **4a^{MIX}**) and 2-chloro-“spiro”-4,4-pentamethylene-1,3,2-oxathiaphospholane (for **4b^{MIX}**), followed by sulfurization with elemental sulfur. Monomers **4a^{MIX}** and **4b^{MIX}**, obtained as mixtures of P-diastereomers, were synthesized in satisfactory yields of 65% and 68%, respectively.

The identities of both compounds were confirmed by HRMS, with the corresponding spectra provided in Fig. S13 and S14 (SI). The next step involved developing conditions for the separation of the monomers into pure diastereomers. It turned out that the P-diastereomers of **4a^{MIX}** could be successfully separated using a silica gel cartridge (FP EcoFlex Si 12 g) in a flash chromatography system (Fig. S15, SI). However, the mixture of **4b^{MIX}** diastereomers was separated *via* preparative HPLC (Fig. S16, SI) using a Pursuit XRs silica gel column. Baseline separation of the P-diastereomers was successfully achieved using the eluents listed in Table 1. Their diastereomeric purity was confirmed through ^{31}P NMR, 1H NMR, and ^{13}C NMR (Fig. S17–28, SI).



Scheme 2 Unexpected results of the phosphorylation of an N -hydroxymorpholino derivative (mU^{OH}).

Molecular modeling experiments: computational analysis of $N-O-P$ vs. $N-N-P$ bond stability

A key question is whether we could rationalize why the synthetic pathway leading to the $N-O-P$ formation (Scheme 2) is not stable, while the formation of the $N-N-P$ derivative seems to result in a stable compound. To explore this, we investigated the relative stability of $N-O$ and $N-N-P$ bonds using quantum chemical calculations. We performed calculations on both $N-O-P$ and $N-N-P$ model compounds using Gaussian software,²⁹ and assessed their stability through bond order analysis with the Multiwfn program.³⁰ Bond order provides a quantitative measure of bond strength and is widely employed to understand molecular electronic structures and to predict stability or reactivity. Numerous definitions of bond order have been proposed in the literature.^{31–34} In this study, we performed two types of bond order analysis: Intrinsic Bond Strength Index



Table 1 Chromatographic and spectroscopic characteristics of *N*-aminomorpholino oxathiaphospholane monomers **4a** and **4b** and their P-diastereomers (**4a**^{Fast} and **4a**^{Slow}, **4b**^{Fast} and **4b**^{Slow})

OTP	4a	4b
Yield ^a (%)	65	68
<i>R</i> _f ^b (TLC)	0.71	0.74
Eluent for separation (v/v)	Hexane : ethyl acetate (70 : 30) ^c	Hexane : ethyl acetate (60 : 40) ^d
MM calc. (Da)	682	750
HR MS (<i>m/z</i>) ^e	681.1602	749.2220
P-diastereomers	Fast (4a ^{Fast})	Slow (4a ^{Slow})
<i>R</i> _t (min)	22	28
δ ³¹ P NMR (ppm) ^f	96.04	96.05
	Fast (4b ^{Fast})	Slow (4b ^{Slow})

^a Yield of the isolated mixture of P-diastereomers. ^b CHCl₃ : MeOH (9 : 1). ^c Cartridge packed with silica gel of a flash chromatography system (Reveleris), flow rate 5 mL min⁻¹, isocratic elution. ^d Pursuit XRs silica gel HPLC column, 10 μ m, 250 mm \times 21.2 mm, flow rate 5 mL min⁻¹, isocratic elution. ^e Recorded with a SYNAPT G2-Si High Definition Mass Spectrometer. ^f In anhydrous CD₃CN.

(IBSI)³⁵ and Laplacian Bond Order (LBO),³⁶ both of which are efficient and reliable tools for evaluating bond strength. For the N–O–P and N–N–P models, the calculated values were IBSI = 0.62 and LBO = 0.16 for the N–O bond, and IBSI = 0.79 and LBO = 0.57 for the N–N bond, respectively.

These differences between the two bonds suggest significantly greater stability for the N–N–P bond compared to the N–O–P bond. Although quantum chemical calculations cannot serve as definitive proof, they strongly support the hypothesis of inherent instability of the N–O–P bond. Fig. 4 shows the graphical representation of the energy calculated bond orders and molecular structures of the N–O–P and N–N–P models, clearly illustrating the weaker bonding interaction in the N–O–P system compared to the more stable N–N–P analog.

X-ray crystallography analysis of the oxathiaphospholane monomer

In order to gain detailed structural insights into the stereochemistry of these novel P-stereodefined *N*-aminomorpholino analogs, we conducted X-ray crystallographic studies on the crystallized form of the mU-^NOTP monomer (compound **4a**^{Fast}). For the first time, we present the crystal structure of a separated P-diastereomer of an *N*-aminomorpholino monomer, with its absolute configuration unambiguously determined (*S*_P, Fig. 5). These structural data not only confirm the stereochemical outcome of the oxathiaphospholane methodology but also serve as a valuable reference for future studies on the structure–activity relationships (SAR) of an expanded class of P-stereodefined nucleic acid analogs.

Crystallization attempts using DMT-protected OTP derivatives were unsuccessful, likely due to the bulky and hydrophobic nature of the dimethoxytrityl group, which interferes with crystal packing and solvent interactions. Drawing on previous experience with the crystallization of oxathiaphospholane derivatives in both DNA¹⁷ and LNA¹⁸ series, where DMT deprotection of 5'-OH significantly improved crystallization success, we decided to remove the DMT protecting group from the mU-^NOTP monomers. Detritylation was performed under mild, anhydrous conditions in acetonitrile, using a suspension

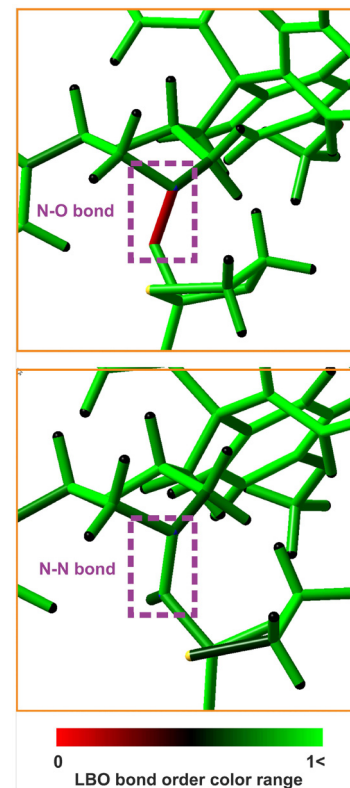


Fig. 4 Color visualization of the calculated LBO bond orders and molecular structures for the N–O–P and N–N–P models. The discussed bonds are highlighted with a violet dashed rectangle.

of sodium hydrogen sulfate supported on silica gel.³⁷ This approach underscores the importance of strategic protecting group manipulation when working with stereochemically complex nucleotide analogs.

Following purification, the resulting 6'-OH deprotected monomers (**4a**^{Fast}, **4a**^{Slow}, **4b**^{Fast} and **4b**^{Slow}) were subjected to crystallization trials. Crystals suitable (only for **4a**^{Fast}) for single-crystal X-ray diffraction analysis were successfully obtained *via* slow solvent evaporation under ambient con-



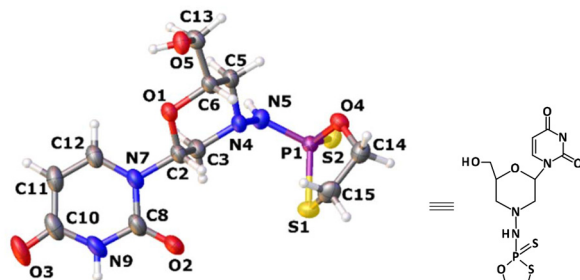


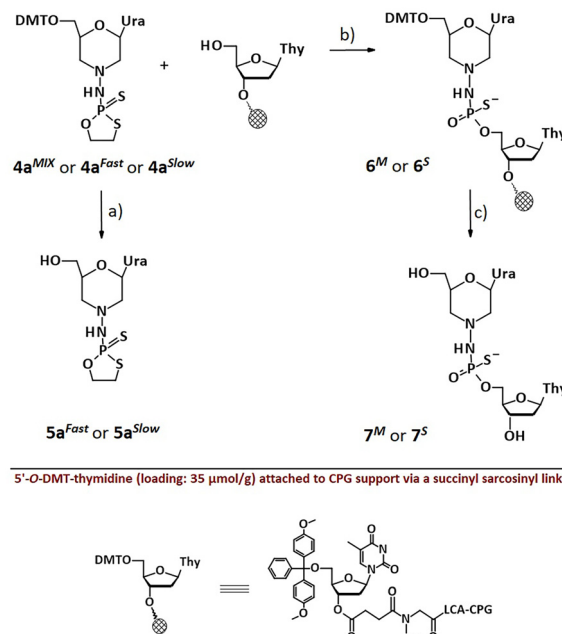
Fig. 5 ORTEP diagram (X-ray crystallography) of the fast-eluting 6'-OH P-diastereomer of $4\mathbf{a}^{\text{Fast}}$, confirming the S_P absolute configuration. Atom color scheme: red – oxygen, blue – nitrogen, yellow – sulfur, purple – phosphorus. CCDC deposition number: 2470809.

ditions. Colourless crystals of compound $4\mathbf{a}^{\text{Fast}}$ in the shape of thick plates were obtained by recrystallization from a 7:2:1 (v/v/v) mixture of chloroform, acetonitrile and hexane. A crystal of $4\mathbf{a}^{\text{Fast}}$, measuring $0.25 \times 0.15 \times 0.05 \text{ mm}^3$, was selected and mounted on an appropriate support. Data collection was carried out at a constant temperature of 100 K using a Rigaku XtaLAB Synergy-S Dualflex diffractometer equipped with a HyPix-6000HE detector. The structure was resolved using the intrinsic phasing method implemented in the ShelXT³⁸ structure solution program, with Olex2³⁹ serving as the graphical interface. Refinement of the structural model was carried out using the least-squares minimization method in ShelXL⁴⁰ (version 2018/3). The crystal data and refinement parameters for $4\mathbf{a}^{\text{Fast}}$ are collected in Table S2 (SI).

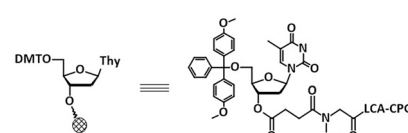
The fast-eluting derivative of $4\mathbf{a}$ crystallized in the monoclinic $P2_1$ space group with two molecules of the compound in the asymmetric unit. In addition, partially occupied and disordered molecules of acetonitrile and chloroform used for crystallization were identified (Fig. S38, SI).

Solid-phase synthesis of *N*-aminomorpholino dinucleoside phosphorothioate ($\text{mU}_{\text{NPS}}\text{T}$) via the oxathiaphospholane strategy

We decided to evaluate the efficiency of the oxathiaphospholane strategy using solid-phase synthesis to construct internucleotide phosphorothioate linkages with *N*-aminomorpholino nucleosides, aiming to demonstrate its potential as a robust method for the synthesis of P-stereodefined oligonucleotide analogs. The introduction of *N*-aminomorpholino oxathiaphospholane monomers marks a significant advancement in the development of modified phosphorothioates, providing a robust platform for expanding the database of P-stereodefined oligonucleotides. To investigate the applicability of nucleophilic bases previously²⁵ used in our studies, namely DBU, TBD and Verkade's base, we conducted a series of coupling experiments aimed at synthesizing *N*-aminomorpholino dinucleoside phosphorothioate. The *N*-aminomorpholino oxathiaphospholane monomers ($4\mathbf{a}^{\text{MIX}}$ and $4\mathbf{b}^{\text{MIX}}$ as a mixture of P-diastereomers) were reacted with thymidine attached to a solid support, resulting in the formation of the dinucleotide



5'-O-DMT-thymidine (loading: 35 $\mu\text{mol/g}$) attached to CPG support via a succinyl sarcosinyl linker



Scheme 4 The synthesis of the dinucleoside phosphorothioate $\text{mU}_{\text{NPS}}\text{T}$. Conditions: (a) cat. $\text{NaHSO}_4/\text{SiO}_2$ in CH_3CN ; (b) 1.5 eq. activator, 2 eq. 3'-O-Ac-Thy, anhydrous acetonitrile; and (c) 1 step: 1.5% dichloroacetic acid (DCA) in CH_2Cl_2 ; 2 step: NH_4OH , 18 h, rt.

analog 6'OH- $\text{mU}_{\text{NPS}}\text{T-OH}$ (Scheme 4). As previously reported, in the case of morpholino analogs,²⁵ the use of the standard 1 M DBU protocol resulted in a significant decrease in coupling efficiency, even when double coupling was applied during the condensation steps, with yields dropping to 61%, as determined by the DMT^+ cation assay. In contrast, using a 3 M solution of TBD in acetonitrile markedly improved the yield of the double coupling step to approximately 93%. The highest repetitive condensation efficiency, however, was observed when using 2 M Verkade's base (Vb), reaching up to 95% according to the DMT^+ cation assay (Table 2).

However, for the *N*-aminomorpholino oxathiaphospholane monomers, the coupling yields were even higher. When using DBU, TBD, or Verkade's base as an activator, the efficiencies were comparable and they consistently exceeded 90% for all three bases (Fig. S34–S36, SI). As shown in Table 1, the initial

Table 2 Coupling yields with OTP monomers in solid phase synthesis of dimers 6^M calculated from the DMT^+ decay assay

OTP monomer	Standard OTP method DBU ^a	Modified OTP method	
		TBD ^b	Verkade ^c
$4\mathbf{a}^{\text{MIX}}$	95 ^{dc}	93 ^{dc}	94
$4\mathbf{b}^{\text{MIX}}$	>95		

dc, double coupling. ^a 1 M DBU solution in anhydrous acetonitrile. ^b 3 M TBD solution in anhydrous acetonitrile. ^c 2 M Verkade solution in anhydrous acetonitrile.

condensation reactions with a 2'-deoxynucleoside anchored to a solid support proceeded with the desired efficiency (>90%) for both **4a^{MIX}** and **4b^{MIX}** monomers. Notably, oxathiaphospholane derivatives of *N*-aminomorpholino nucleosides exhibited reactivity closely matching that of standard oxathiaphospholane derivatives of 2'-deoxynucleosides and 2'-O-TBDMS-ribonucleosides, achieving yields exceeding 90% using the standard OTP methodology. As in the case of 2'-O-TBDMS monomers, a double-condensation step was necessary to achieve optimal yields. This stands in contrast to morpholino analogs, which in our previous work required the development of new activators to achieve satisfactory coupling efficiencies.^{25,26} In the present study, the conventional and cost-effective DBU proved entirely sufficient, enabling high-yielding couplings without additional optimization. This observation strongly suggests that these compounds may not only behave analogously to standard phosphorothioates in synthesis but could also share their favorable biochemical properties, making them attractive candidates for further exploration in oligonucleotide design.

The isolated dimers (**7^M**) were subsequently subjected to enzymatic and chemical stability assays to evaluate their structural integrity under biologically relevant conditions.

Based on these results, we also performed the synthesis of a P-stereodefined dimer using the slow-eluting diastereomer (**4a^{Slow}**). After cleavage from the solid support, the products were purified by semi-preparative RP-HPLC (Fig. S30, SI), affording the target dinucleoside phosphorothioate. Purified **7^S** was analyzed by analytical RP-HPLC (Fig. S31, SI) and confirmed by HRMS (Fig. S32, SI).

These studies are crucial for evaluating the potential of new modified oligonucleotide analogs as therapeutic candidates, particularly with regard to enhancing their stability, bioavailability, and efficacy within biological systems.

Toward therapeutic potential: enzymatic stability of P-stereodefined *N*-aminomorpholino phosphorothioates

Synthetic oligonucleotides represent a significant class of therapeutic agents with great potential.⁴¹ However, to fully appreciate the therapeutic potential of newly synthesized derivatives, it is essential to check their degradability *in vivo* by nucleases while ensuring their stability for participation in other cellular processes. To evaluate the potential biological applications of P-stereodefined *N*-modified morpholino phosphorothioate analogs, we conducted degradation studies in fetal bovine serum (FBS), a commonly used supplement in animal cell cultures.

Fetal bovine serum contains a variety of nucleases capable of hydrolyzing pyrophosphate and phosphodiester bonds, as well as nutrients that closely mimic the intracorporeal environment.⁴² It has been widely used to evaluate the stability of modified nucleotides and oligonucleotides under physiologically relevant conditions. As serum-based systems reflect many aspects of the physiological environment, they offer a robust platform for assessing the enzymatic resistance of modified oligonucleotides.

To assess the stability of compound **7^M** under physiologically relevant conditions, the dinucleotide was incubated in a 10% (v/v) FBS solution at 37 °C. Aliquots were taken at various time points and analyzed by RP HPLC (Fig. S37, SI). Samples were collected after 24 and 72 hours of incubation. HPLC analysis showed no detectable degradation of the compound, indicating that the dimer remains stable under these serum-containing conditions over an extended period. The stability profile of the investigated compound is fully consistent with the well-established behavior of the phosphorothioate class of modified backbones.

To further assess the stability of the dinucleotide **7^M**, an additional enzymatic assay was conducted. In this experiment, **7^M** was treated with nuclease P1 (nP1), which specifically cleaves the *S_P*-configuration,⁴³ and snake venom phosphodiesterase (svPDE), which preferentially targets substrates with the *R_P*-configuration.⁴⁴ After a 24-hour incubation at 37 °C with either nP1 or svPDE, the dinucleotide was analyzed by RP-HPLC (Fig. 6). Both stereoisomers of **7^M** displayed exceptional resistance to enzymatic degradation. This result supports the conclusion that P-stereodefined morpholino phosphorothioate analogs possess exceptional resistance to enzymatic degradation, consistent with the behavior previously observed for morpholino phosphorothioate analogs.⁴⁵

Toward therapeutic potential: chemical stability of P-stereodefined *N*-aminomorpholino phosphorothioates

Additionally, the chemical stability of the dinucleotide was evaluated across a broad pH range (5–9) to simulate different physiological and extreme conditions. The incubation conditions and buffer compositions are summarized in Table S1. Samples were incubated for 24 hours at 37 °C in the following media: acetate buffer (pH 5), phosphate-buffered saline (PBS, pH 7.4), and Tris-HCl buffer (pH 9). After incubation, the samples were analyzed by RP-HPLC. No degradation was observed under any of the tested conditions, indicating that the dinucleotide maintains its structural integrity in both enzymatic and chemically challenging environments. These results suggest that compound **7^M** exhibits a high degree of resistance to enzymatic cleavage and is well-suited for potential biological or therapeutic applications.

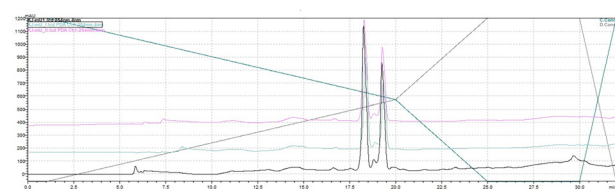


Fig. 6 HPLC profiles of reaction solutions after treatment of **7^M** with nP1 (green line) and svPDE (pink line) over 24 h at 37 °C; RP-HPLC was performed with a linear gradient of 0%–40% CH_3CN in 0.1 M TEAB buffer (pH 7.3) over 32 min at a rate of 0.5 mL min^{-1} . Description: black line, dinucleotide **7^M** (formed from a mixture of P-diastereomers) without enzymes.



Conclusions

In conclusion, the findings of this study confirm that the oxathiaphospholane methodology represents a highly effective strategy for the stereocontrolled synthesis of novel P-stereodefined phosphorothioate N-modified morpholino analogs. Oxathiaphospholane derivatives of *N*-aminomorpholino nucleosides (mU-^NOTP) were synthesized in high yields and successfully separated into pure P-diastereomers. Crystallographic analysis demonstrated that the fast-eluting mU-^NOTP corresponds to the *S_P* diastereomer.

To evaluate the stability of the synthesized analogs under biologically relevant conditions, we conducted stability assays in fetal bovine serum. The results indicated favorable stability in an environment that mimics *in vivo* conditions. These results facilitated the insightful investigation of the stability of P-stereodefined *N*-aminomorpholino phosphorothioates in serum, providing some crucial information for future clinical research and pharmacological studies.

Although preliminary, these results suggest that the novel N-modified morpholino OTP monomers show considerable potential for the development of next-generation antisense oligonucleotides. To our satisfaction, the studied *N*-aminomorpholino phosphorothioate analogs exhibited reactivity comparable to standard thiophosphates, without the need for any modifications to the OTP method. In contrast to morpholino analogs, which in our previous work^{25,26} required the use of novel activators, the conventional and cost-effective DBU proved fully sufficient here, enabling high-yielding synthesis. This observation strongly suggests that these compounds may behave similarly to standard phosphorothioates.

Further in-depth studies are planned to fully explore their therapeutic potential. Future efforts will focus on the synthesis of stereodefined N-modified morpholino phosphorothioate oligonucleotides incorporating other nucleobases. This strategy is expected to deepen our understanding of their structural versatility and broaden their applicability in targeted therapeutic approaches.

Author contributions

K. J. supervised the project as well as prepared and edited the manuscript. K. J. and A. S. performed the chemical syntheses and data analysis. R. D. conducted crystallization, crystal diffraction data collection and analysis. T. P. performed quantum chemical calculations and data analysis. All authors reviewed and approved the final version of the manuscript.

Conflicts of interest

The authors declare no competing financial interest.

Data availability

The data supporting this article have been included as part of the SI: detailed experimental procedures and associated data. See DOI: <https://doi.org/10.1039/d5ob01223f>.

CCDC 2470809 contains the supplementary crystallographic data for this paper.⁴⁶

Acknowledgements

This work was financially supported by the National Centre of Science, Poland, grant 2021/43/D/ST4/02433 (to K. J.). An Avance Neo 400 NMR spectrometer and Rigaku XtaLAB Synergy-S X-Ray diffractometer systems were purchased using funds provided by the EU Regional Operational Program of the Łódź Region RPLD.01.01.00-10-0008/18.

The authors are grateful to Professor Arkadiusz Chworus (CMMS PAS) for constructive suggestions and discussions.

Katarzyna Jastrzębska expresses gratitude to Professor Marvin H. Caruthers (University of Colorado Boulder) for scientific inspiration and continuous support.

References

- 1 (a) A. Kumari and R. K. Singh, Morpholine as ubiquitous pharmacophore in medicinal chemistry: Deep insight into the structure-activity relationship (SAR), *Bioorg. Chem.*, 2020, **96**, 103578; (b) A. P. Kourounakis, D. Xanthopoulos and A. Tzara, Morpholine as a privileged structure: A review on the medicinal chemistry and pharmacological activity of morpholine containing bioactive molecules, *Med. Res. Rev.*, 2020, **40**, 709–752.
- 2 B. Selvakumar, S. P. Vaidyanathan, M. Subbiah and K. P. Elango, Synthesis and antiviral activity of 4-(7,7-dimethyl-4-[4-{N-aryl/benzyl}1-piperazinyl]-5,6,7,8-tetrahydro quinazolin-2-yl)morpholine derivatives, *ARKIVOC*, 2017, 353–364.
- 3 F. Arshad, M. F. Khan, W. Akhtar, M. M. Alam, L. M. Nainwal, S. K. Kaushik, M. Akhter, S. Parvez, S. M. Hasan and M. Shaquiquzzaman, Revealing quinquennial anticancer journey of morpholine: a SAR based review, *Eur. J. Med. Chem.*, 2019, **167**, 324–356.
- 4 E. Lenci, L. Calugi and A. Trabocchi, Occurrence of Morpholine in Central Nervous System Drug Discovery, *ACS Chem. Neurosci.*, 2021, **12**, 378–390.
- 5 J. Summerton and D. Weller, Morpholino antisense oligomers: design, preparation, and properties, *Antisense Nucleic Acid Drug Dev.*, 1997, **7**, 187–195.
- 6 Q. Ge, M. Pastey, D. Kobasa, P. Puthavathana, C. Lupfer, R. K. Bestwick, P. L. Iversen, J. Chen and D. A. Stein, Inhibition of multiple subtypes of influenza A virus in cell cultures with morpholino oligomers, *Antimicrob. Agents Chemother.*, 2006, **50**, 3724–3733.



7 Y. Xiong, T. J. McQuistan, J. W. Stanek, J. E. Summerton, J. E. Mata and T. C. Squier, Detection of unique Ebola virus oligonucleotides using fluorescently-labeled phosphorodiamide morpholino oligonucleotide probe pairs, *Anal. Biochem.*, 2018, **557**, 84–90.

8 A. Sakai, G. Singh, M. Khoshbakht, S. Bittner, C. V. Löhr, R. Diaz-Tapia, P. Warang, K. White, L. Le Luo, B. Tolbert, M. Blanco, A. Chow, M. Guttman, C. Li, Y. Bao, J. Ho, S. Maurer-Stroh, A. Chatterjee, S. Chanda, A. García-Sastre, M. Schotsaert, J. R. Teijaro, H. M. Moulton and D. A. Stein, Inhibition of SARS-CoV-2 growth in the lungs of mice by a peptide-conjugated morpholino oligomer targeting viral RNA, *Mol. Ther. – Nucleic Acids*, 2024, **35**, 1–16.

9 S. M. Daly, C. R. Sturge and D. E. Greenberg, Inhibition of Bacterial Growth by Peptide-Conjugated Morpholino Oligomers, *Methods Mol. Biol.*, 2017, **1565**, 115–122.

10 H. M. Moulton and J. D. Moulton, Morpholinos and their peptide conjugates: Therapeutic promise and challenge for Duchenne muscular dystrophy, *Biochim. Biophys. Acta, Mol. Basis Dis.*, 2010, **12**, 2296–2303.

11 H. Langner, K. Jastrzebska and M. Caruthers, Synthesis and Characterization of Thiophosphoramidate Morpholino Oligonucleotides and Chimeras, *J. Am. Chem. Soc.*, 2020, **142**, 16240–16253.

12 (a) G. Dumbović, U. Braunschweig, H. K. Langner, M. Smallegan, J. Biayna, E. P. Hass, K. Jastrzebska, B. Blencowe, T. R. Cech, M. H. Caruthers and J. L. Rinn, Nuclear compartmentalization of TERT mRNA and TUG1 lncRNA is driven by intron retention, *Nat. Commun.*, 2021, **12**, 3308–3326; (b) G. Dumbović, H. Krishna, K. Jastrzebska, M. Caruthers and J. L. Rinn, Method for retaining splicing RNAs in the nucleus based on chemically modified antisense oligonucleotides, US 2021/015673, 2021.

13 (a) B. T. Le, S. Paul, K. Jastrzebska, H. Langer, M. H. Caruthers and R. N. Veedu, Thiomorpholino oligonucleotides as a robust class of next generation platforms for alternate mRNA splicing, *Proc. Natl. Acad. Sci. U. S. A.*, 2022, **119**, 1–8; (b) M. Caruthers, S. Paul, R. N. Veedu, K. Jastrzebska and H. Krishna, Thiomorpholino oligonucleotides for the treatment of Duchene muscular dystrophy, US 2023/0193266-A1, 2023.

14 N. Iwamoto, D. C. D. Butler, N. Svrzikapa, S. Mohapatra, I. Zlatev, D. W. Y. Sah, S. Meena, S. M. Standley, G. Lu, L. H. Apponi, M. Frank-Kamenetsky, J. J. Zhang, C. Vargeese and G. L. Verdine, Control of phosphorothioate stereochemistry substantially increases the efficacy of antisense oligonucleotides, *Nat. Biotechnol.*, 2017, **35**, 845–851.

15 W. Liu, N. Iwamoto, S. Marappan, K. Luu, S. Tripathi, E. Purcell-Estabrook, J. D. Shelke, H. Shah, A. Lamattina, Q. Pan, B. Schrand, F. Favaloro, M. Bedekar, A. Chatterjee, J. Desai, T. Kawamoto, G. Lu, J. Metterville, M. Samaraweera, P. S. Prakasha, H. Yang, Y. Yin, H. Yu, P. H. Giangrande, M. Byrne, P. Kandasamy and C. Vargeese, Impact of stereopure chimeric backbone chemistries on the potency and durability of gene silencing by RNA interference, *Nucleic Acids Res.*, 2023, **51**, 4126–4147.

16 W. J. Stec, A. Grajkowski, M. Koziołkiewicz and B. Uznański, Novel route to oligo(deoxyribonucleoside phosphorothioates). Stereocontrolled synthesis of P-chiral oligo(deoxyribonucleoside phosphorothioates), *Nucleic Acids Res.*, 1991, **19**, 5883–5888.

17 W. J. Stec, B. Karwowski, M. Boczkowska, P. Guga, M. Koziołkiewicz, M. Sochacki, M. W. Wieczorek and J. Błaszczyk, Deoxyribonucleoside 3'-O-(2-Thio- and 2-Oxo-“spiro”-4,4-pentamethylene-1,3,2-oxathiaphospholane)s: Monomers for Stereocontrolled Synthesis of Oligo(deoxyribonucleoside phosphorothioate)s and Chimeric PS/PO Oligonucleotide, *J. Am. Chem. Soc.*, 1998, **120**, 7156–7167.

18 K. Jastrzebska, A. Maciaszek, R. Dolot, G. Bujacz and P. Guga, Thermal Stability and Conformation of Antiparallel Duplexes Formed by P-Stereodefined Phosphorothioate DNA/LNA Chimeric Oligomers with DNA and RNA Matrices, *Org. Biomol. Chem.*, 2015, **13**, 10032–10040.

19 K. Jastrzebska, B. Mikołajczyk and P. Guga, LNA units present in $[R_p\text{-PS}]\text{-}(\text{DNA}\#\text{LNA})$ chimeras enhance the thermal stability of parallel duplexes and tripleplexes formed with (2'-OMe)-RNA strands, *RSC Adv.*, 2020, **10**, 22370–22376.

20 A. Tomaszewska-Antczak, K. Jastrzebska, A. Maciaszek, B. Mikołajczyk and P. Guga, P-Stereodefined phosphorothioate, analogs of glycol nucleic acids – synthesis and structural properties, *RSC Adv.*, 2018, **8**, 24942–24952.

21 K. Jastrzebska, A. Maciaszek, R. Dolot, A. Tomaszewska-Antczak, B. Mikołajczyk and P. Guga, Synthesis and hybridizing properties of P-stereodefined chimeric $[\text{PS}]\text{-}(\text{DNA:RNA})$ and $[\text{PS}]\text{-}(\text{DNA:}(2'\text{-OMe})\text{-RNA})$ oligomers, *RSC Adv.*, 2022, **12**, 26815–26824.

22 E. Radzikowska, R. Kaczmarek, D. Korczyński, A. Krakowiak, B. Mikołajczyk, J. Baraniak, P. Guga, K. A. Wheeler, T. Pawlak and B. Nawrot, P-stereocontrolled synthesis of oligo(nucleoside N3'→O5' phosphoramidothioate)s – opportunities and limitations, *RSC Adv.*, 2020, **10**, 35185–35197.

23 (a) S. Gryaznov, T. Skorski, C. Cucco, M. Nieborowska-Skorska, C. Y. Chiu, D. Lloyd, J. K. Chen, M. Koziołkiewicz and B. Calabretta, *Nucleic Acids Res.*, 1996, **24**, 1508–1514; (b) S. M. Gryaznov, *Biochim. Biophys. Acta*, 1999, **1489**, 131–140; (c) T. Skorski, D. Perrotti, M. Nieborowska-Skorska, S. M. Gryaznov and B. Calabretta, *Proc. Natl. Acad. Sci. U. S. A.*, 1997, **94**, 3966–3971.

24 (a) S. Gryaznov, K. Pongracz, T. Matray, R. Schultz, R. Pruzan, J. Aimi, A. Chin, C. Harley, B. Shea-Herbert, J. Shay, Y. Oshima, A. Asai and Y. Yamashita, Telomerase inhibitors – oligonucleotide phosphoramidates as potential therapeutic agents, *Nucleosides, Nucleotides Nucleic Acids*, 2001, **20**, 401–449; (b) R. Pruzan, K. Pongracz, K. Gietzen, G. Wallweber and S. M. Gryaznov, Allosteric inhibitors of telomerase: oligonucleotide N3'→P5' phosphoramidates, *Nucleic Acids Res.*, 2002, **30**, 559–568.



25 K. Jastrzębska, An efficient alternative to DBU in the oxathiaphospholane (OTP) method for the solid phase synthesis of P-stereodefined phosphorothioate analogs, *RSC Adv.*, 2024, **14**, 21174–21179.

26 K. Jastrzębska, P. Antończyk and R. Dolot, P-Stereodefined, morpholino dinucleoside 3',5'-phosphorothioates, *Org. Biomol. Chem.*, 2024, **22**, 8737–8742.

27 (a) Y. V. Tarasenko, T. V. Abramova, V. I. Mamatuk and V. N. Silnikov, Effective Synthesis of Fluorescently Labeled Morpholino Nucleoside Triphosphate Derivatives, *Nucleosides, Nucleotides Nucleic Acids*, 2016, **35**, 32–42; (b) N. Debreczeni, J. Hotzi, M. Bege, M. Lovas, E. Mező, I. Bereczki, P. Herczegh, L. Kiss and A. Borbas, *N*-Fluoroalkylated, Morpholinos – a New Class of Nucleoside Analogues, *Chem. – Eur. J.*, 2023, **29**, 1–15.

28 K. Jastrzębska, A. Szymańska and A. Chworoś, Oksatiafosfolanowe pochodne N-aminomorfolinowych nukleozydów oraz P-stereozdefiniowane tiofosforanowe analogi N-aminomorfolinowych kwasów nukleinowych, sposób ich wytwarzania oraz ich zastosowanie, PL452641, WIPO ST 10/C PL452641, 2025.

29 M. J. Frisch, G. W. Trucks, H. B. Schlegel, G. E. Scuseria, M. A. Robb, J. R. Cheeseman, G. Scalmani, V. Barone, G. A. Petersson, H. Nakatsuji, X. Li, M. Caricato, A. V. Marenich, J. Bloino, B. G. Janesko, R. Gomperts, B. Mennucci, H. P. Hratchian, J. V. Ortiz, A. F. Izmaylov, J. L. Sonnenberg, D. Williams-Young, F. Ding, F. Lipparini, F. Egidi, J. Goings, B. Peng, A. Petrone, T. Henderson, D. Ranasinghe, V. G. Zakrzewski, J. Gao, N. Rega, G. Zheng, W. Liang, M. Hada, M. Ehara, K. Toyota, R. Fukuda, J. Hasegawa, M. Ishida, T. Nakajima, Y. Honda, O. Kitao, H. Nakai, T. Vreven, K. Throssell, J. A. Montgomery Jr., J. E. Peralta, F. Ogliaro, M. J. Bearpark, J. J. Heyd, E. N. Brothers, K. N. Kudin, V. N. Staroverov, T. A. Keith, R. Kobayashi, J. Normand, K. Raghavachari, A. P. Rendell, J. C. Burant, S. S. Iyengar, J. Tomasi, M. Cossi, J. M. Millam, M. Klene, C. Adamo, R. Cammi, J. W. Ochterski, R. L. Martin, K. Morokuma, O. Farkas, J. B. Foresman and D. J. Fox, *Gaussian 16, Revision C.01*, Gaussian, Inc., Wallingford CT, 2019.

30 T. Lu and F. Chen, Multiwfns: A multifunctional wavefunction analyzer, *J. Comput. Chem.*, 2012, **33**, 580–592.

31 A. E. Reed and P. v. R. Schleyer, Chemical Bonding in Hypervalent Molecules. The Dominance of Ionic Bonding and Negative Hyperconjugation over d-Orbital Participation, *J. Am. Chem. Soc.*, 1990, **112**, 1434–1445.

32 K. B. Wiberg, Application of the Pople–Santry–Segal CNDO Method to the cyclopropylcarbinyl and Cyclobutyl Cation and to Bicyclobutane, *Tetrahedron*, 1968, **24**, 1083–1096.

33 I. Mayer, Charge, Bond Order and Valence in the Ab Initio SCF Theory, *Chem. Phys. Lett.*, 1983, **97**, 270–274.

34 A. Michalak, R. L. DeKock and T. Ziegler, Bond Multiplicity in Transition-Metal Complexes: Applications of Two-Electron Valence Indices, *J. Phys. Chem. A*, 2008, **112**, 7256–72639.

35 J. Klein, H. Khartabil, J. C. Boisson, J. Contreras-García, J. P. Piquemal and E. Hénon, New Way for Probing Bond Strength, *J. Phys. Chem. A*, 2020, **124**, 1850–1860.

36 T. Lu and F. Chen, Bond Order Analysis Based on the Laplacian of Electron Density in Fuzzy Overlap Space, *J. Phys. Chem. A*, 2013, **117**, 3100–3108.

37 R. K. Kannasani, V. V. S. Peruri and S. R. Battula, $\text{NaHSO}_4\text{-SiO}_2$ as an efficient and chemoselective catalyst, for the synthesis of acylal from aldehydes under, solvent-free conditions, *Chem. Cent. J.*, 2012, **6**, 136.

38 G. M. Sheldrick, SHELXT - Integrated space-group and crystal-structure determination, *Acta Crystallogr., Sect. A: Found. Adv.*, 2015, **71**, 3–8.

39 L. J. Bourhis, O. V. Dolomanov, R. J. Gildea, J. A. K. Howard and H. Puschmann, The anatomy of a comprehensive constrained, restrained refinement program for the modern computing environment - Olex2 dissected, *Acta Crystallogr., Sect. A: Found. Adv.*, 2015, **71**, 59–75.

40 G. M. Sheldrick, Crystal structure refinement with SHELXL, *Acta Crystallogr., Sect. C: Struct. Chem.*, 2015, **71**, 3–8.

41 C. A. Stein and D. Castanotto, FDA-Approved Oligonucleotide Therapies in 2017, *Mol. Ther.*, 2017, **25**, 1069–1075.

42 J. W. Conway, C. K. McLaughlin, K. J. Castor and H. Sleiman, DNA nanostructure serum stability: greater than the sum of its parts, *Chem. Commun.*, 2013, **49**, 1172–1174.

43 B. V. L. Potter, B. A. Connolly and F. Eckstein, Synthesis and configurational analysis of a dinucleoside phosphate isotopically chiral at phosphorus. Stereochemical course of *Penicillium citrum* nuclease P1 reaction, *Biochemistry*, 1983, **22**, 1369–1377.

44 (a) P. M. J. Burgers and F. Eckstein, Absolute configuration of the diastereomers of adenosine 5'-0-(1-thiotriphosphate): Consequences for the stereochemistry of polymerization by DNA-dependent RNA polymerase from *Escherichia coli*, *Proc. Natl. Acad. Sci. U. S. A.*, 1978, **75**, 4798–4801; (b) P. M. J. Burgers, F. Eckstein and D. H. Hunneman, Stereochemistry of hydrolysis by snake venom phosphodiesterase, *J. Biol. Chem.*, 1979, **254**, 7476–7478.

45 K. Jastrzębska and A. Chworoś, Oksatiafosfolanowe pochodne morfolinowych nukleozydów oraz P-stereozdefiniowane tiofosforanowe analogi morfolinowych kwasów nukleinowych, sposób ich wytwarzania i zastosowanie, PL446811, WIPO ST 10/C PL446811, 2023.

46 K. Jastrzębska, A. Szymańska, T. Pawlak and R. Dolot, CCDC 2470809: Experimental Crystal Structure Determination, 2025, DOI: [10.5517/ccdc.csd.cc2ny2j7](https://doi.org/10.5517/ccdc.csd.cc2ny2j7).

